

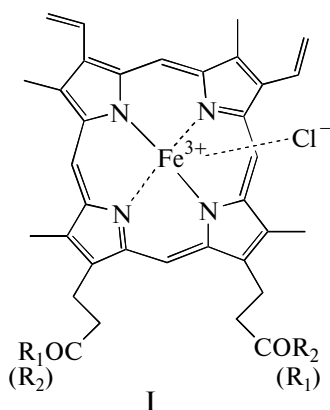
Relationship between Self-Organization, Physicochemical Properties, and Biological Activity of Aqueous Solutions of Hemin Derivatives

I. S. Ryzhkina, Yu. V. Kiseleva, G. A. Zheltukhina, S. A. Okorochkov, L. I. Murtazina, A. P. Timosheva, V. E. Nebolsin, and Academician A. I. Kononov^a

Received May 27, 2011

DOI: 10.1134/S0012501611090016

It was recently found that synthetic derivatives of hemin, a natural metalloporphyrin, modified with amino acid and peptide residues of general formula **I** have antitumor, virucidal, and other biological activity [1, 2]. The effective concentration range for many hemin derivatives is 10^{-6} – 10^{-4} mol/L. Nowadays, a major trend in the search for efficient antitumor agents is the creation of drugs with a high therapeutic index, low toxicity, and minimal side effects, which can be achieved by means of decreasing the effective concentrations.



II: $R_1 = R_2 = \text{SerOMe}$

III: $R_1 = R_2 = \text{ArgOMe}$

Combined study of characteristics of aqueous solutions of different biologically active compounds

*Arbuzov Institute of Organic and Physical Chemistry,
Kazan Research Center, Russian Academy of Sciences,
ul. Akademika Arbuzova 8,
Kazan, 420083 Tatarstan, Russia*
*Lomonosov Moscow State Academy
of Fine Chemical Technology,
pr. Vernadskogo 86, Moscow, 119571 Russia*
*Pharmenterprises OOO, pr. Vernadskogo 86,
Moscow, 119571 Russia*

(BACs) as a function of concentration [3–7] has demonstrated that BAC solutions of low and ultralow concentration are self-organizing systems containing nanosized (100–300 nm) associates (nanoassociates) with a negative surface charge. Dilution of solutions by the serial dilution method leads to nonlinear changes in nanoassociate parameters (size, ζ -potential), as well as in physicochemical properties of solutions. The extreme values of nanoassociate parameters, solution characteristics, and bioeffects are observed in nearly the same concentration ranges of BAC solutions [4–7]. This makes it possible to predict the appearance of the bioeffect in highly diluted aqueous solutions of BACs [8].

The aim of this work was to reveal specific features of self-organization of highly diluted aqueous solutions of two hemin derivatives (**II** and **III**) in a concentration range of 10^{-17} – 10^{-3} mol/L, study concentration dependences of physicochemical properties of hemin derivative solutions (electric conductivity, surface tension, dielectric constant), and establish the relationship between the associate parameters, physicochemical properties, and physiological activity of hemin derivative solutions.

Our findings demonstrated that the replacement of the amino acid residue serine (**II**) by arginine (**III**) in the molecule of hemin derivative **I** leads to a significant change in the aggregation behavior, physicochemical properties, and biological activity of solutions of these compounds so that the effective concentration increases from 2×10^{-5} to 8×10^{-5} mol/L for solutions of **II** and **III**, respectively. The antitumor activity of solutions of **II** and **III** correlates with the degree of accumulation of aggregates of hemin derivatives in solution. These aggregates are likely a major active principle of the observed biological activity of solutions of compounds **II** and **III** in the concentration range 10^{-6} – 10^{-4} mol/L. Comparison of the nonlinear concentration dependences of nanoassociate parameters and physicochemical properties of highly diluted solutions (10^{-18} – 10^{-7} mol/L) of **II** and **III**

pointed to the possibility of tailored design of hemin derivatives with different ability for self-organization in solutions of ultralow concentration (10^{-18} – 10^{-13} mol/L). On the basis of the previously discovered tendencies [3–8], we predicted the appearance of the bioeffect of solutions of **III** in the ranges 10^{-12} – 10^{-11} and 10^{-15} – 10^{-17} mol/L.

Compounds **II** and **III** were synthesized as described in [2]. The mass spectrometric and IR and UV-Vis spectroscopic data were consistent with those reported in [2]. The self-organization of aqueous solutions of hemin derivatives was studied by UV-Vis spectroscopy, dynamic light scattering, microelectrophoresis, tensiometry, conductometry, pH-metry, and dielectric permittivity measurements. Working solutions of **II** and **III** were prepared by the serial dilution method from a starting 1×10^{-2} M aqueous solution. For water insoluble compound **II**, working aqueous solutions containing 1 vol % DMSO were prepared from an initial 1×10^{-3} M solution in DMSO. Freshly prepared double distilled water with a conductivity of no more than $1.5 \mu\text{S}/\text{cm}$ was used for preparing solutions.

The size (effective hydrodynamic diameter of a kinetically mobile particle at the maximum of the distribution curve, D) and the ζ -potential of associates were measured by the dynamic light scattering (DLS) and electrophoresis on a highly sensitive Zetasizer Nano ZS analyzer (Malvern Instruments). In the double distilled water used, the analyzer fixed no particles. Aqueous solutions of **III** showed a unimodal particle size distribution in the entire concentration range of 10^{-18} – 10^{-3} mol/L. Study of the self-organization of solutions of **II** is complicated by the formation of clusters 200 nm in size in a mixed water–DMSO solvent containing 1 vol % DMSO. In this case, the concentration dependences were plotted and the subsequent analysis of the experimental data was performed using only systems with unimodal particle size distribution in the range of concentrations of **II** 1×10^{-11} – 1×10^{-5} mol/L in which the particle size was other than 200 nm, i.e., differed from the size of solvent clusters. Particles of such size formed in solutions of **II** at a concentration of 1×10^{-12} mol/L and lower.

The surface tension (σ), electric conductivity (χ), and pH of solutions were measured on a high-precision Sigma 720ET tensiometer (KSV Instruments) and an inoLab Cond Level 1 conductometer at $25 \pm 0.1^\circ\text{C}$. The dielectric permittivity (ϵ) of solutions was measured at 298 K on a setup consisting of an E12-1 instrument operating by the beat method and a measuring cell comprising a capacitor maintained at a constant temperature. The electronic absorption spectra of solutions of hemin derivatives were recorded on a Helios Gamma spectrophotometer (Thermo Electron). The relative errors of measurement were as follows: for the particle size in solutions of compounds **II** and **III**, 5–15%; for the ζ -potential, 4–20%; for the

surface tension, 1–2.5%; for the electric conductivity and dielectric permittivity of solutions, 5–12%. The errors of measurement depended on the solution concentration and solute.

To obtain information on possible aggregation processes in solutions of hemin derivatives in the concentration range 1×10^{-6} – 1×10^{-4} mol/L, electronic absorption spectra of solutions were recorded in the range 300–650 nm. The molar absorption coefficient (k) at the maxima of absorption bands was calculated from the equation $\log(I/I_0) = kcd$, where $\log(I/I_0)$ is the absorbance at the absorption band maximum, c is the molar concentration of a hemin derivative, and d is the cell thickness (in centimeters).

The electronic absorption spectra of 1×10^{-6} M solutions of **II** and **III** show two bands at 350 and 396 nm. As the concentration of **III** increases to 5×10^{-5} mol/L, the molar extinction coefficients decrease and the bands are hypsochromically shifted, which can be an indication of formation of aggregates, including H-type aggregates [9, 10]. In the spectra of solutions of **II**, an increase in the concentration is additionally accompanied by band broadening, which is evidence of a larger variety of associates of **II** as compared with **III**. With a further increase in the concentration of **II** and **III** in solutions, the k values change nonlinearly, which supports the conclusion of aggregation processes that occur in the concentration range 10^{-6} – 10^{-4} mol/L [9, 10]. The change in the concentration of **III** in an aqueous solution from 1×10^{-6} to 1×10^{-5} mol/L is accompanied by the largest changes in k , which testifies to the most significant structural rearrangements in solution in this concentration range. For solutions of **II** and **III**, the lowest extinction coefficient is observed at a concentration of 5×10^{-5} mol/L; this hypochromism can reflect the maximal degree of ordering of molecules in the associate [10].

The self-organization of solutions of **II** and **III** in a wider concentration range, including ultralow concentrations, was studied by DLS (Fig. 1a) and electrophoresis (Fig. 1b). Joint analysis of concentration dependences of the size and ζ -potential of the associates forming in solutions of **II** and **III** allows us to conventionally divide the entire range of concentrations under consideration into two overlapping segments where sharp changes in the concentration dependences and associate parameter values occur: the segments of common and low concentrations. For solutions of **II**, the first segment is 3×10^{-5} – 1×10^{-6} mol/L and the second segment is 1×10^{-7} – 1×10^{-11} mol/L; for solutions of **III**, these segments are 3×10^{-3} – 1×10^{-5} and 1×10^{-6} – 1×10^{-18} mol/L, respectively.

For both solutions, the first segment (common concentrations) is characterized first of all by a sharp decrease in the ζ -potential of associates, which nearly reaches a plateau by the beginning of the second segment. In solutions of **II**, the ζ -potential drops from –

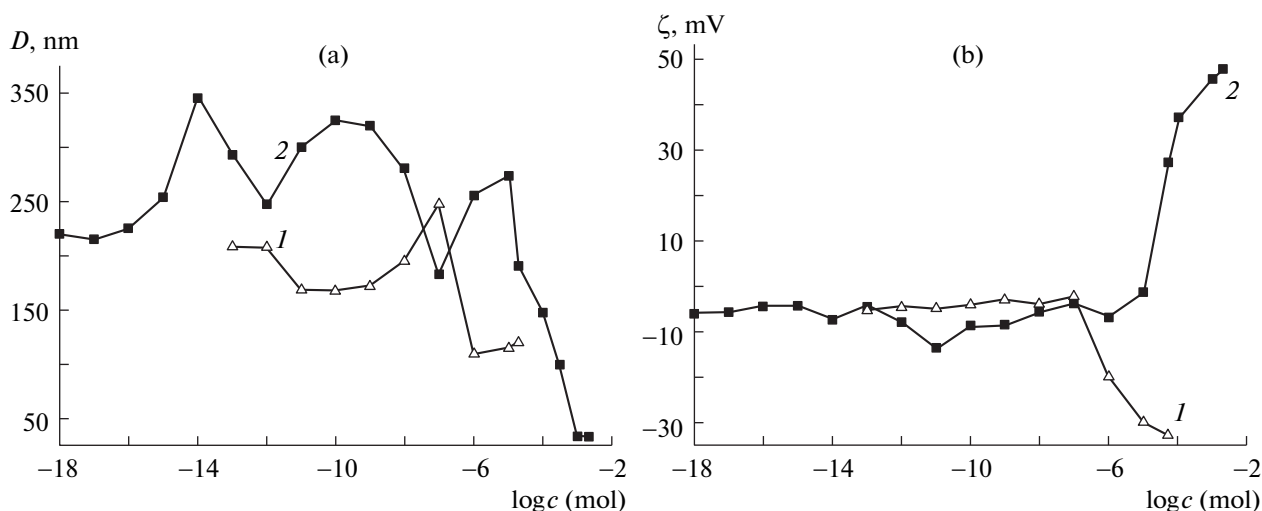


Fig. 1. (a) Particle size and (b) ζ -potential as a function of concentration of hemin derivatives (1) **II** and (2) **III** in solutions.

33 to -2 mV in the range 3×10^{-5} – 1×10^{-7} mol/L and in solutions of **III**, from $+45$ to -2 mV in the range 3×10^{-3} – 1×10^{-5} mol/L. The size of associates in solutions of **II** in the common concentration range changes slightly, being ~ 120 nm, whereas the size of associates in solutions of **III** increases by nearly an order of magnitude: from 25 to 276 nm. These results point to a considerable difference in the structure and opposite charges of the particles forming in solutions of **II** and **III** in the common concentration range.

In solutions of low and ultralow concentrations (second segment), the nanoassociate size changes nonlinearly with dilution from 170 to 250 nm for **II** and from 175 to 350 nm for **III**. It is worth noting that formation of nanoassociates in solutions of **III** occurs in a much wider concentration range, including 10^{-18} mol/L, whereas in solutions of **II**, the aggregation ends at 10^{-11} mol/L. At lower concentrations of **II**, there are only clusters of the mixed solvent of ~ 200 nm in size.

The ζ -potential value as a function of concentration nonlinearly changes from -2 to -5 mV for solutions of **II** in the range 1×10^{-7} – 1×10^{-11} mol/L and from -3 to -15 mV for solutions of **III** in the range 1×10^{-6} – 1×10^{-18} mol/L. Thus, small differences in the structure between hemin derivatives **II** and **III** have a rather significant effect not only on the aggregation behavior of solutions in the common concentration range but also on the self-organization of highly diluted solutions of these compounds. This is evidence that tailored design of hemin derivatives will make them promising for preparing highly diluted aqueous solutions in which nanoassociates will form at ultralow concentrations.

Figure 2 shows the plots of the electric conductivity and surface tension of solutions of **II** and **III** as a function of solution concentration in a wide range. As is

seen, compound **II** is not a surfactant. On the basis of the UV-Vis spectroscopy, DLS (Fig. 1a), and electrophoresis (Fig. 1b) data, we can conclude that solutions of this compound in the range 1×10^{-6} – 5×10^{-5} mol/L contain negatively charged aggregates ~ 120 nm in size presumably involving “quasi-crystalline” water structures, which impart a negative charge to these species like in [11]. According to DLS, the critical aggregation concentration in a solution of **II** is 1×10^{-6} mol/L.

The data in Figs. 1 and 2 demonstrate that compound **III** is a cationic micellar surfactant with the 5 critical micelle concentration (CMC) of 1×10^{-3} . The size of positively charged micellar aggregates at CMC 5 is 37 nm.

Hence, aggregation, the increase in the aggregate charge, and the concomitant significant change in the

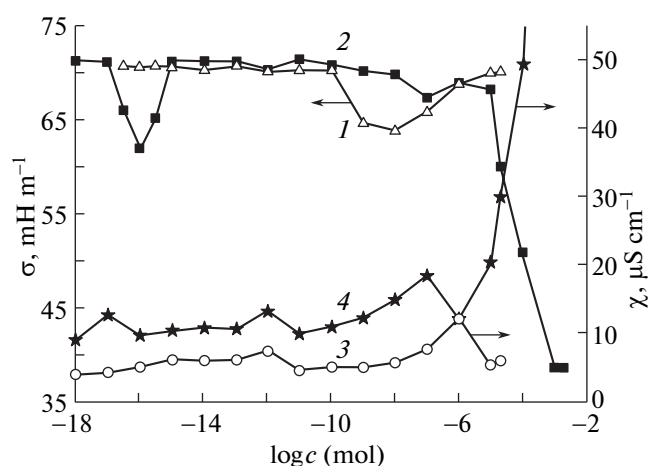


Fig. 2. (1, 2) Surface tension and (3, 4) electric conductivity of solutions of (1, 3) **II** and (2, 4) **III** vs. concentration.

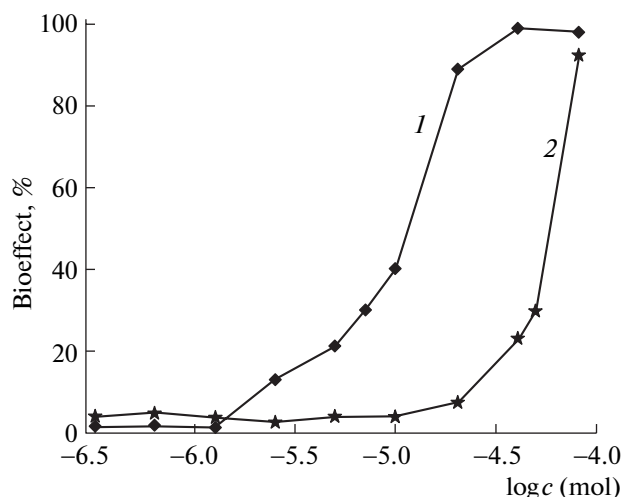


Fig. 3. Inhibition of K562 cell growth vs. the concentration of (1) **II** and (2) **III** in an incubation medium. Incubation conditions: 36 h at 37°C, 5% CO₂, 100% humidity.

physicochemical properties of solutions of **II** occur at lower concentrations than for solutions of **III**. These data are consistent with the antitumor effect of solutions of **II** and **III**. Figure 3 shows the results of studying inhibition of K562 cell growth by solutions of **II** and **III**, which indicate that the same bioeffect is achieved at a higher concentration of **III** as compared with that of **II**. In particular, the 30% cell growth inhibition occurs in a 7×10^{-6} M solution of **II** and in a 5×10^{-5} M solution of **III** (Fig. 3). At the hemin derivative concentration of 5×10^{-5} mol/L, solutions of **II** ensure the maximal (98%) and solutions of **III**, noticeable (30%) inhibition of tumor cell growth. According to DLS, electrophoresis, tensiometry, and conductometry (Figs. 1 and 2), the largest amount of aggregates accumulates in solutions of **II** near this concentration: the aggregate parameters and physicochemical quantities characterizing solution properties reach a plateau.

In 5×10^{-5} M solutions of **III**, a definite amount of micelles also accumulates, which leads to a decrease in the surface tension of solutions to 50 mN/m and an increase in the ζ -potential to +25 mV. However, the aggregate parameters and physicochemical properties of solutions reach a plateau only after the CMC, which is 1×10^{-3} mol/L for **III**; i.e., the largest amount of micellar aggregates accumulates in solutions at considerably higher concentration of **III**. Thus, the antitumor effect of solutions of **II** and **III** observed in the concentration range 10^{-6} – 10^{-4} mol/L correlates with the degree of accumulation of hemin derivative aggregates in solution, which are likely the major active principle of the observed biological activity of solutions of these compounds.

Analysis of the nonlinear concentration dependences of the electric conductivity and surface tension of solutions of **II** and **III** of low and ultralow concentrations (Fig. 2), as well as of the dielectric permittivity of a medium, testifies to the correlation between physicochemical properties of these compounds and self-organization in their solutions (Figs. 1a and 1b). In particular, the local minima in the surface tension isotherm and the increase in the conductivity of solutions of **III** at 1×10^{-7} , 1×10^{-12} , and 1×10^{-16} mol/L reflect a considerable decrease in the nanoassociate size at these concentrations (Fig. 1a).

The local minimum of the surface tension isotherm of solutions of **II** in the range 1×10^{-7} – 1×10^{-10} mol/L is consistent with the decrease in the nanoassociate size in the concentration range 1×10^{-7} – 1×10^{-12} mol/L and the appearance of a local maximum in the plot of the dielectric permittivity versus concentration in this range (Figs. 1a and 2). In addition, in solutions of **II** with concentrations below 1×10^{-12} mol/L where nanoassociates of **II** were not detected, the conductivity and surface tension remain nearly unaltered (Fig. 2), and the concentration dependence of ϵ becomes linear.

The above results confirm the previously revealed relationship between the nonlinear concentration dependences of nanoassociate parameters and physicochemical properties of BAC solutions of low and ultralow concentrations [3–7]. The method of bioeffect prediction in highly diluted aqueous solutions of BACs [8] allows us to suggest that aqueous solutions of **III** are candidates for further study of such effects on the range of low and ultralow concentrations.

ACKNOWLEDGMENTS

We are grateful to A.A. Ignatova and A.S. Maslova (Institute of Bioorganic Chemistry, RAS, Moscow) for studying the antitumor activity of hemin derivatives **II** and **III** against K562 cells.

This work was supported by the Russian Foundation for Basic Research (project no. 10–03–00147) and the Ministry of Education and Science of the Russian Federation (Analytical Departmental Targeted Program “Development of Scientific Potential of the Higher School” 2.1.1/2889).

REFERENCES

1. Zheltukhina, G.A., Nebol'sin, V.A., Nossik, N.N., and Zheltukhin, S.L., Abstracts of Papers, *V International Conference on Porphyrins and Phthalocyanines, Moscow, 6–11 July, 2008*, Moscow, 2008, p. 63.
2. RF Patent No. 2280649, *Byull. Izobret.*, No. 21 (2006).
3. Ryzhkina, I.S., Murtazina, L.I., Kiseleva, Yu.V., and Kononov, A.I., *Dokl. Phys. Chem.*, 2009, vol. 428,

- part 2, pp. 196–200 [*Dokl. Akad. Nauk*, 2009, vol. 428, no. 4, pp. 487–491].
4. Ryzhkina, I.S., Murtazina, L.I., Kiseleva, Yu.V., and Kononov, A.I., *Dokl. Phys. Chem.*, 2009, vol. 428, part 2, pp. 201–205 [*Dokl. Akad. Nauk*, 2009, vol. 428, no. 5, pp. 628–632].
 5. Ryzhkina, I.S., Murtazina, L.I., Sherman, E.D., et al., *Dokl. Phys. Chem.*, 2010, vol. 433, part 2, pp. 142–146 [*Dokl. Akad. Nauk*, 2010, vol. 433, no. 5, pp. 647–651].
 6. Ryzhkina, I.S., Kiseleva, Yu.V., Murtazina, L.I., et al., *Dokl. Phys. Chem.*, 2011, vol. 438, part 2, pp. 109–113 [*Dokl. Akad. Nauk*, 2011, vol. 438, no. 5, pp.].
 7. Ryzhkina, I.S., Murtazina, L.I., Sherman, E.D., et al., *Dokl. Phys. Chem.*, 2011, vol. 438, part 1, pp. 98–102 [*Dokl. Akad. Nauk*, 2011, vol. 438, no. 2, pp. 207–211].
 8. Kononov, A.I., Ryzhkina, I.S., and Murtazina, L.I., *Byul. Izobret.*, 2010, no. 24.
 9. Perevoshchikova, N.B. and Mal'tseva, A.N., *Vestn. Udmurt. Univ.*, 2008, no. 2, pp. 97–106.
 10. Blinova, I.A. and Vasil'ev, V.V., *Zh. Neorg. Khim.*, 1998, vol. 43, no. 12, pp. 2005–2009.
 11. Andrievsky, G.V., Bruskov, V.I., Tykhomyrov, A.A., and Gudkov, S.V., *Free Radical Biol. Med.*, 2009, vol. 47, pp. 786–793.

SPELL: 1. virucidal, 2. arginine, 3. inoLab, 4. nanoassociates, 5. micellar